

identical by HPLC, TLC, ^{13}C NMR, and, most importantly, by 400-MHz ^1H NMR (in CH_2Cl_2 solution) with an authentic specimen. Synthetic dolastatin 10 also exhibited the same level (ED_{50} 10^{-4} $\mu\text{g}/\text{mL}$) of activity against the P388 lymphocytic leukemia as routinely obtained with the natural product.

The preceding total synthetic solutions to the dolastatin 10 stereochemical and availability problems will now greatly accelerate preclinical development, synthesis of potentially useful structural and chiral modifications, and a broad assessment of biological properties.

Acknowledgment. Very necessary financial support was provided by the Fannie E. Rippel Foundation, the Arizona Disease Control Research Commission, Herbert K. and Dianne Cummings (The Nathan Cummings Foundation, Inc.), Eleanor W. Libby, the Waddell Foundation (Donald Ware), Grant CA-16049-10-12 awarded by the National Cancer Institute, and DHHS and NSF equipment Grants CHE-8211164, CHE-8620177 (to the University of Nebraska, Midwest Center for Mass Spectrometry), and CHE-8409644. We also thank Drs. Y. Kamano, C. L. Herald, and C. Dufresne and Chemetals, Maryland, for their assistance.

Registry No. 1, 110417-88-4; 2b, 120205-48-3; 2b (*N-Z* derivative), 120205-58-5; 2b (*N-Z*, 3-OH derivative), 120294-43-1; (3*S*,4*S*,5*S*)-2b (*N-Z*, 3-OH derivative), 120205-57-4; 3, 120205-49-4; 4a-TFA, 120205-63-2; 4b, 120205-50-7; 4b ((*S*)-CHPhCHPh₂ ester), 120294-47-5; 4b (3'-OH, (*S*)-CHPhCHPh₂ ester), 120294-46-4; (2*S*,2'*S*,3'*R*)-4b (3'-OH, (*S*)-CHPhCHPh₂ ester), 120205-60-9; (2*S*,2'*S*,3'*S*)-4b (3'-OH, (*S*)-CHPhCHPh₂ ester), 120294-44-2; (2*S*,2'*R*,3'*S*)-4b (3'-OH, (*S*)-CHPhCHPh₂ ester), 120294-45-3; (2*S*,2'*S*,3'*R*)-4b ((*S*)-CHPhCHPh₂ ester), 120205-61-0; 5, 120205-51-8; (2*S*,6*S*)-5b (2,3,4,5-tetrahydro derivative), 120205-64-3; (2*R*,6*S*)-5b (2,3,4,5-tetrahydro derivative), 120205-65-4; 6, 120205-52-9; 7, 120205-53-0; 8, 120205-54-1; Z-Ile-OH, 3160-59-6; (*S,S*)-ZnMeCH(CHMeEt)CH₂OH, 120205-55-2; (*S,S*)-ZnMeCH(CHMeEt)CHO, 120205-56-3; AcOBu-*t*, 540-88-5; BOC-Pro-OH, 15761-39-4; (*S*)-CH₂CH₂COOCHPhCHPh₂, 120205-59-6; BOC-Phe-OH, 13734-34-4; (*S*)-(BOC)NHCH(CH₂Ph)CHO, 72155-45-4; H₂NCH₂CH₂SH, 60-23-1; Z-Val-OH, 1149-26-4; Dov-OPfp, 97800-78-7; BOC-(*S*)-prolinal, 69610-41-9.

Supplementary Material Available: X-ray crystal structure determination summary (including tables of distances and angles and coordinates and an ORTEP drawing) for the lactam derived from (2*S*,2'*S*,3'*R*)-dolaproine (8 pages). Ordering information is given on any current masthead page.

The Electron Affinity of (η^4 -1,3-Butadiene)iron Tricarbonyl, η^4 -Bd-Fe(CO)₃

G. W. Dillow, G. Nicol, and P. Kebarle*

Department of Chemistry, University of Alberta
Edmonton, Alberta, Canada T6G 2G2

Received January 6, 1989

Although formation of negative ions in the gas phase from organometallic compounds has long been known,^{1,2} only very limited information is currently available on the electron affinities of organometallic species. Electron affinities have been determined by laser photodetachment for simple metal carbonyls such as $\text{Fe}(\text{CO})_4$ ³ and $\text{Ni}(\text{CO})_4$,⁴ but very little is known about the electron affinities of more complex substituted metal carbonyls.

In this communication we report the first determination of the free energy of electron attachment, ($-\Delta G^\circ_a \approx \text{EA}$), for η^4 -Bd-Fe(CO)₃ by pulsed high pressure mass spectrometry (PHPMS). PHPMS has been shown to be highly suitable for the determination of EAs of molecules which undergo resonance electron

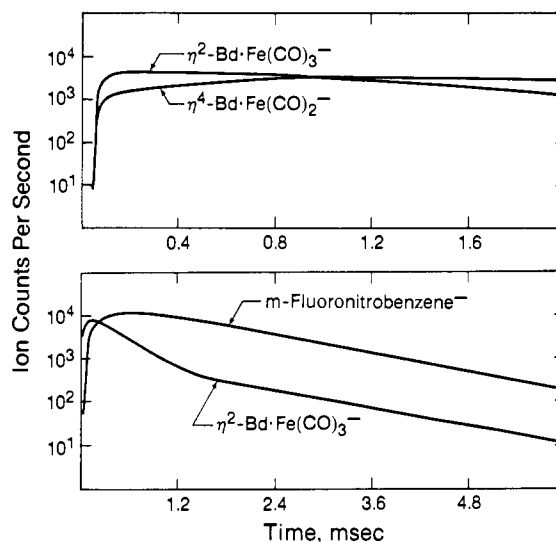
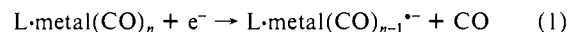
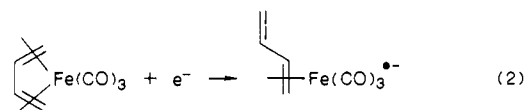


Figure 1. (top) Time profiles for the η^2 -Bd-Fe(CO)₃⁻ and η^4 -Bd-Fe(CO)₂⁻ produced in a mixture of 2.6 mTorr η^4 -Bd-Fe(CO)₃ in 6 Torr methane; 10 μs electron pulse. (bottom) Time profile for the molecular ions produced in a mixture containing 12.9 mTorr η^4 -Bd-Fe(CO)₃ and 17.1 mTorr *m*-fluoronitrobenzene in methane (6 Torr) following a 100- μs electron pulse. Both experiments at 150 °C temperature.

capture and has been used to determine the EAs of a wide variety of organic compounds.⁵ While the majority of metal carbonyls undergo dissociative electron capture, reaction 1, rather than



resonance electron capture in order to avoid violation of the 18-electron rule,^{1,2} certain substituted metal carbonyls bearing tetra- and hexahaptate ligands may undergo resonance electron capture by reducing the hapticity of the ligand.⁶⁻⁹ A well-known example is η^4 -Bd-Fe(CO)₃ which forms the stable 17-electron anion, η^2 -Bd-Fe(CO)₃⁻, as shown in reaction 2.^{6,8,9} Studies of the equivalent



reduction in solution, where the product ion may be fully characterized, have confirmed the dihapto coordination of the butadiene ligand and indicated that the negative charge is located largely on the metal.¹⁰

The PHPMS experiments with η^4 -Bd-Fe(CO)₃ were performed with instrumentation that has been described in detail previously,⁵ with standard experimental conditions. Chemical reactions were initiated by directing 10–100 μs pulses of energetic (2000 V) electrons into methane gas maintained at 6 Torr pressure and 150 °C and containing mTorr quantities of the reactants. Product ions which diffused from the ion source through a narrow orifice were accelerated, mass selected, and collected by a multichannel analyzer as a function of time after the initiating electron pulse.

With η^4 -Bd-Fe(CO)₃ present as the only reactant in the methane mixture, an abundant molecular ion, η^2 -Bd-Fe(CO)₃⁻, was observed along with a fragment ion identified as η^4 -Bd-Fe(CO)₂⁻. Figure 1 shows the time profiles of these ions for a period of 2 ms after the electron pulse. It is evident that under our experimental conditions, the η^2 -Bd-Fe(CO)₃⁻ molecular ion undergoes a slow unimolecular loss of CO (rate constant $\approx 600 \text{ s}^{-1}$) to

(5) Kebarle, P.; Chowdhury, S. *Chem. Rev.* 1987, 87, 513.

(6) Blake, M. R.; Garnett, J. L.; Gregor, I. K.; Wild, S. B. *J. Chem. Soc., Chem. Commun.* 1979, 496.

(7) Blake, M. R.; Garnett, J. L.; Gregor, I. K.; Wild, S. B. *J. Organomet. Chem.* 1979, 178, C37.

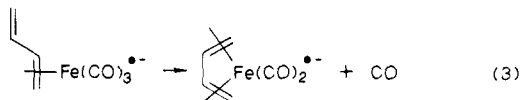
(8) McDonald, R. N.; Schell, P. L.; Chowdhury, A. K. *J. Am. Chem. Soc.* 1985, 107, 5578.

(9) Wang, D.; Squires, R. R. *Organometallics* 1987, 6, 905.

(10) Krusic, P. J.; San Filippo, J., Jr. *J. Am. Chem. Soc.* 1982, 104, 2645.

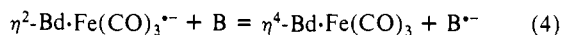
(1) Gregor, I. K.; Guilhaus, M. *Mass Spectrom. Rev.* 1984, 3, 32.
(2) Squires, R. R. *Chem. Rev.* 1987, 87, 623.
(3) Engelking, P. C.; Lineberger, W. C. *J. Am. Chem. Soc.* 1979, 101, 5569.
(4) Stevens, A. E.; Feigerle, C. S.; Lineberger, W. C. *J. Am. Chem. Soc.* 1982, 104, 5026.

produce the $\eta^4\text{-Bd}\cdot\text{Fe}(\text{CO})_2^{\bullet-}$ ion. It is envisaged that the uncoordinated butadiene double bond in the molecular ion recoordinates to the metal and displaces a CO molecule as shown in reaction 3. Since electron capture by $\eta^4\text{-Bd}\cdot\text{Fe}(\text{CO})_3$ results in



cleavage of an Fe-alkene bond rather than an Fe-CO bond, it appears that reaction 3 must be endothermic and is driven by the entropy gain of the dissociation (3). Measurements of the rate of (3) at higher temperatures led, via an Arrhenius plot, to an activation energy, $E_3 \approx 20$ kcal/mol. Further experiments¹¹ involving the equilibrium 3 indicated that E_3 is close to the enthalpy change ΔH_3 .

The free energy of electron attachment to $\eta^4\text{-Bd}\cdot\text{Fe}(\text{CO})_3$, $\Delta G^\circ_a[\eta^4\text{-Bd}\cdot\text{Fe}(\text{CO})_3]$, was determined by measuring the equilibrium constant for electron-transfer reaction 4, K_4 , where B corresponds to reference molecules nitrobenzene, *p*-fluoronitrobenzene, or *m*-fluoronitrobenzene. The free energies for electron attachment to these reference molecules, $\Delta G^\circ_a(\text{B})$, have been determined previously to be -22.8, -25.0, and -27.7 kcal mol⁻¹, respectively. Upon determination of ΔG°_4 for each electron-transfer equilibrium according to eq 5, $\Delta G^\circ_a[\eta^4\text{-Bd}\cdot\text{Fe}(\text{CO})_3]$ was calculated by inserting the appropriate values of ΔG°_4 and $\Delta G^\circ_a(\text{B})$ into eq 6. Figure 1 shows a pair of ion time profiles



$$\Delta G^\circ_4 = -RT \ln K_4 \quad (5)$$

$$\Delta G^\circ_a[\eta^4\text{-Bd}\cdot\text{Fe}(\text{CO})_3] = \Delta G^\circ_a(\text{B}) - \Delta G^\circ_4 \quad (6)$$

obtained during these experiments. In this particular case $\eta^2\text{-Bd}\cdot\text{Fe}(\text{CO})_3^{\bullet-}$ was the predominant ion present shortly after the electron pulse, but its intensity decreased steadily due to electron transfer to *m*-fluoronitrobenzene until, after approximately 2 ms, equilibrium was achieved as evidenced by the parallel ion plots, and K_4 was calculated from the constant ion ratio observed beyond this point. A series of experiments where P_A/P_B was progressively changed by a factor of 10 led to K_4 values which were independent of the pressure ratio as expected from eq 5. From the average value of K_4 for each reference compound, ΔG°_4 was calculated to be +2.5, +0.4, and -2.4 kcal mol⁻¹, respectively, for electron transfer from $\eta^2\text{-Bd}\cdot\text{Fe}(\text{CO})_3^{\bullet-}$ to nitrobenzene, *p*-fluoronitrobenzene, and *m*-fluoronitrobenzene. These values lead via eq 6 to $\Delta G^\circ_a[\eta^4\text{-Bd}\cdot\text{Fe}(\text{CO})_3] = -25.3, -25.4, \text{ and } -25.3$ kcal mol⁻¹, respectively, and an overall mean of -25.3 kcal mol⁻¹.

An interesting feature of the time profiles shown in Figure 1 is the very slow approach to equilibrium which is evident in the first 2 ms. This slow approach to equilibrium corresponds to a rate of electron transfer from $\eta^2\text{-Bd}\cdot\text{Fe}(\text{CO})_3^{\bullet-}$ to *m*-fluoronitrobenzene of only 5×10^{-12} cm³ molecule⁻¹ s⁻¹, even though this reaction is exoergic by 2.4 kcal mol⁻¹. Since exoergic electron-transfer reactions in the gas phase frequently proceed at the collisionally determined maximum rate of $\approx 2 \times 10^{-9}$ cm³ molecule⁻¹ s⁻¹,⁵ it is evident that electron transfer from $\eta^2\text{-Bd}\cdot\text{Fe}(\text{CO})_3^{\bullet-}$ to *m*-fluoronitrobenzene is highly inefficient. This is probably associated with the large difference in structure between $\eta^2\text{-Bd}\cdot\text{Fe}(\text{CO})_3^{\bullet-}$ and $\eta^4\text{-Bd}\cdot\text{Fe}(\text{CO})_3$. Slow rates of electron transfer caused by large structural changes have been identified previously.¹²

More elaborate measurements including variable temperatures, currently in progress,¹¹ indicate, via van't Hoff plots of reaction 4, that the ΔS_2° value for the electron capture (2) is consistent with the expected increased freedom of internal rotation in the $\eta^2\text{-Bd}\cdot\text{Fe}(\text{CO})_3^{\bullet-}$ product ion. Details of these and additional related results will be given in a forthcoming publication.¹¹

(11) Dillow, G. W.; Kebarle, P. manuscript in preparation.

(12) Grimrud, E. P.; Chowdhury, S.; Kebarle, P. *J. Chem. Phys.* **1985**, *104*, 83, 1059. Chowdhury, S.; Kebarle, P. *Chem. Phys.* **1986**, *85*, 4989.

Proton NMR Detection of Long-Range Heteronuclear Multiquantum Coherences in Proteins: The Complete Assignment of the Quaternary Aromatic ¹³C Chemical Shifts in Lysozyme

Donald G. Davis

Laboratory of Molecular Biophysics
National Institute of Environmental Health
P. O. Box 12233
Research Triangle Park, North Carolina 27709

Received March 3, 1989

The development of reverse detection methods¹ has stimulated a renewed interest in ¹³C NMR of macromolecules.^{2,3} In these experiments ¹³C chemical shifts are determined indirectly by detecting the influence of evolving heteronuclear multiquantum coherences on the magnetization of protons scalar coupled to ¹³C. Although maximum sensitivity is obtained for carbons directly bonded to protons, experiments for ¹H detection of multibond heteronuclear correlations have been developed,⁴⁻⁷ but the sensitivity is less and applications have been limited to small molecules or to isotopically enriched macromolecules.^{8,9} It might appear therefore that ¹³C NMR studies of macromolecules using ¹H detection complement those using direct ¹³C detection, where attention was focused, of necessity, on nonprotonated quaternary carbons.¹⁰ This communication demonstrates to the contrary that the shifts of quaternary carbons in the aromatic rings of proteins can be obtained via ¹H detection with almost the same sensitivity as the protonated carbons and thus be used to completely assign the ¹H¹³C 2D spectra of these carbons in a 4.4 mM solution of lysozyme (MW = 14 300). Our results extend and refine those of Allerhand and co-workers¹⁰ who used chemical modification and titration schemes to make assignments. Of greater significance however is the improvement in sensitivity and attendant reduction in materials and time required to solve the assignment problem.

This experiment succeeds for several reasons. First, almost all the quaternary aromatic carbons in proteins are coupled to ring protons through three-bond trans couplings, that are uniformly about 8 Hz.¹¹ Secondly, sensitivity is limited principally by proton T_2 's. Consequently long-range multiquantum states can be optimally prepared ($I_\alpha S_\beta \sin(\pi J \Delta)$; $\alpha, \beta \neq z$) without serious attenuation by relaxation ($\exp(-\Delta/T_2)$). Thirdly, several peaks in the 2D spectra are multiply correlated, while the one-bond correlations are suppressed (vide infra), thus facilitating the assignment problem. Finally, for lysozyme, all the protonated aromatic ¹³C's and their attached ¹H's have been assigned.^{3,12}

For this particular application, we used the HMQC¹³ sequence: $90^\circ_x(^1\text{H})-\Delta-90^\circ_\phi(^{13}\text{C})-t_1/2-180^\circ_x(^1\text{H})-t_1/2-90^\circ_x(^{13}\text{C})-\Delta-[-\text{acquire}(t_2)]$ with ¹³C decoupling. In addition to providing max-

- (1) Griffey, R. H.; Redfield, A. G. *Quart. Rev. Biophys.* **1987**, *19*, 51.
- (2) Wagner, G.; Brühwiler, D. *Biochemistry* **1986**, *15*, 5839.
- (3) Sklenar, V.; Bax, A. *J. Magn. Reson.* **1987**, *71*, 379.
- (4) Bax, A.; Summers, M. F. *J. Am. Chem. Soc.* **1986**, *108*, 2093.
- (5) Bermel, W.; Griesinger, C.; Kessler, H.; Wagner, K. *Magn. Reson. Chem.* **1987**, *25*, 325.
- (6) Bax, A.; Marion, D. *J. Magn. Reson.* **1989**, *78*, 186.
- (7) Davis, D. G. *J. Magn. Reson.* **1989**, *83*, 212.
- (8) Westler, W. M.; Kainosho, M.; Nagao, H.; Tomonaga, N.; Markley, J. L. *J. Am. Chem. Soc.* **1988**, *110*, 4093.
- (9) Bax, A.; Sparks, S. W.; Torchia, D. A. *J. Am. Chem. Soc.* **1988**, *110*, 7926.
- (10) Allerhand, A. *Methods Enzymol.* **1979**, *61*, 458 and references therein.
- (11) Memory, J. D.; Wilson, N. K. *NMR of Aromatic Compounds*; J. Wiley and Sons: New York, 1982; Chapter 5. The cis coupling between Trp-H₃ and -C₇ is apparently small (<3 Hz) but fortunately ²J between Trp-H₃₁ and -C₇ is ca. 6 Hz. All other geminal ring C-H ²J's here are negligibly small (<3 Hz).
- (12) Redfield, C.; Poulson, F. M.; Dobson, C. M. *Eur. J. Biochem.* **1982**, *128*, 527.
- (13) Bax, A.; Griffey, R. H.; Hawkins, B. L. *J. Magn. Reson.* **1983**, *55*, 301. For absorption mode spectra,^{3,13} $\phi = x, y, -x, -y$, with odd and even acquisitions stored in separate blocks of memory and the FID's alternately added and subtracted in each block (i.e., receiver phase = +, +, -, -).